Electronic Supplementary Material (ESI) for Journal of Materials Chemistry C.

Supporting Information

Organic Cluster with Time-Dependent Color-Tunable Dual Persistent Room-Temperature Phosphorescence

Zijian Chen, Mengke Li, Weidong Qiu, Wentao Xie, Qing Gu and Shi-Jian Su*

State Key Laboratory of Luminescent Materials and Devices and Institute of Polymer Optoelectronic Materials and Devices, South China University of Technology, Guangzhou 510640, China

E-mail: mssjsu@scut.edu.cn

Table of contents

1. Experimental procedures
2. Results and discussion
   2.1 Photophysical properties
   2.2 ONIOM model and computation details
   2.3 Relationship between triplet exciton diffusion and overlap between FMOs
   2.4 Single crystal analysis
3. Materials details
4. Reference

1. Experimental procedures

Chemical structure characterization. ^{1}H and ^{13}C NMR spectra were measured on Bruker NMR spectrometer operating at 600 and 150 MHz, respectively. The samples were dissolved in deuterated chloroform ($CDCl_3$) and measured at ambient temperature. HRMS spectra were obtained using a Bruker maXis impact. HPLC diagrams were obtained using a Agilent1290. Small molecule single crystal X-ray analysis was conducted on Rigaku XtaLAB P2000 FR-X with a rotating copper anode and a Pilatus 200K detector at room temperature.

Photophysical characterization. UV-vis absorption spectra were recorded using Perkin-Elmer Lambda 950-PKA instrument. Fluorescence and phosphorescence spectra were recorded by a FluoroMax-4 spectrofluorometer. Transient PL decay spectrum and temperature dependent PL spectrum of crystal were conducted on FL980 (Edinburgh Instrument). Photoluminescent quantum yields (PLQYs) were measured utilizing an integrating sphere of Hamamatsu absolute PL quantum yield spectrometer (Hamamatsu, C11347-01).

Quantum chemical calculation. Theoretical calculations were performed by using the Gaussian 09 E01 package.[1] The ground state geometries of monomer were optimized in B3LYP(D3)/6-311G* level in gas phase according to density functional theory (DFT). Based on the optimized ground state geometries, time dependence density functional theory (TD-DFT) calculations were conducted in B3LYP(D3)/6-311G* level to study the excited state characters.[2-4] Dimer, tetramer and cluster structures were extracted form single crystal XRD results. Before calculation, restricted geometry optimization was conducted in B3LYP(D3)/6-311G* level by "freezing" all atoms except for hydrogen. The T_1 excited state geometries were optimized using ONIOM method in B3LYP(D3)/6-311G* level for central molecular and PM7 for surrounding molecules by "freezing" all surrounding molecules. And based on the optimized ground state geometries of the central molecular, the excited state energies were calculated using TDDFT in B3LYP(D3)/6-311G* level using background electrons to replace the surrounding molecules. And the background electrons were obtained using Restrained Electro Static Potential (RESP) analysis[5] with Multiwfn. The natural transition orbitals (NTOs) and Independent Gradient Model (IGM)[6] were analyzed using Multiwfn and visualized with VMD software.[7, 8] The SOC matrix were calculated with PySOC.[9]

2. Results and discussion

2.1 Photophysical properties

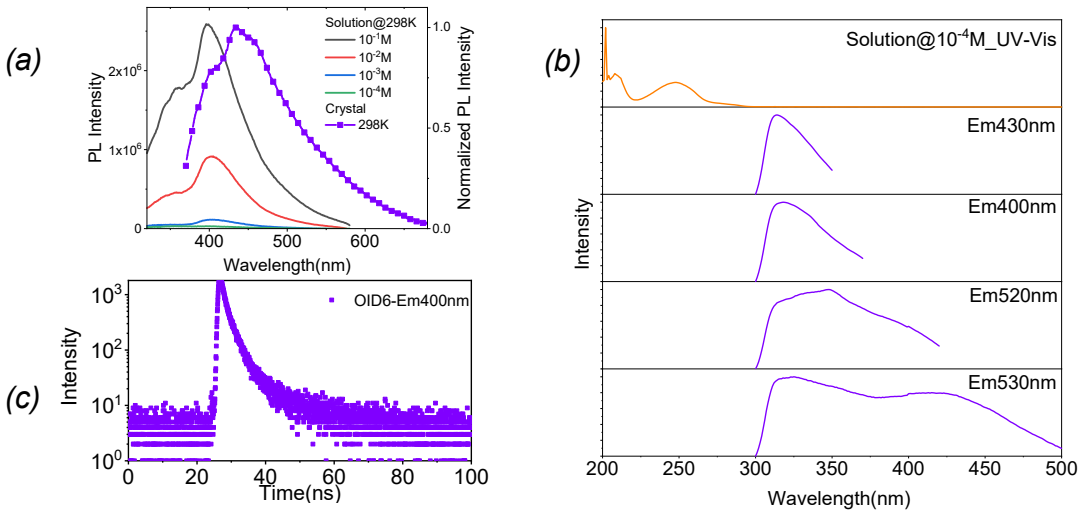

Fig. S1 (a) PL spectra of OID6 in CH_3CN solution at different concentrations and in crystalline state at 298 K; (b) UV-vis absorption spectra of OID6 in 10^{-4} M CH_3CN solution and excitation dependence spectra in crystalline state at 298 K; (c) Transient PL spectra in crystalline state.

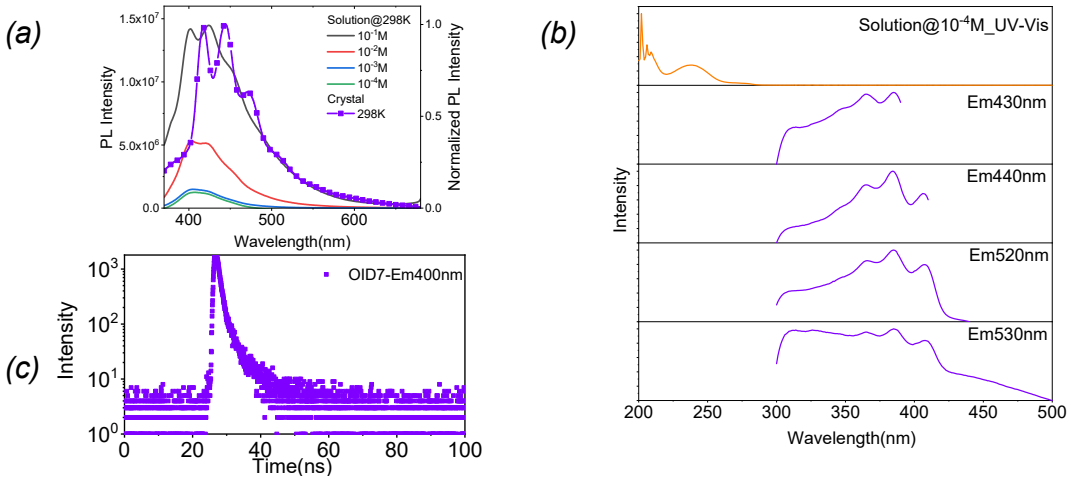

Fig. S2 (a) PL spectra of OID-7 in CH_3CN solution at different concentrations and in crystalline state at 298 K; (b) UV-vis absorption spectra of OID-7 in 10^{-4} M CH_3CN solution and excitation dependence spectra in crystalline state at 298 K; (c) Transient PL spectra in crystalline state.

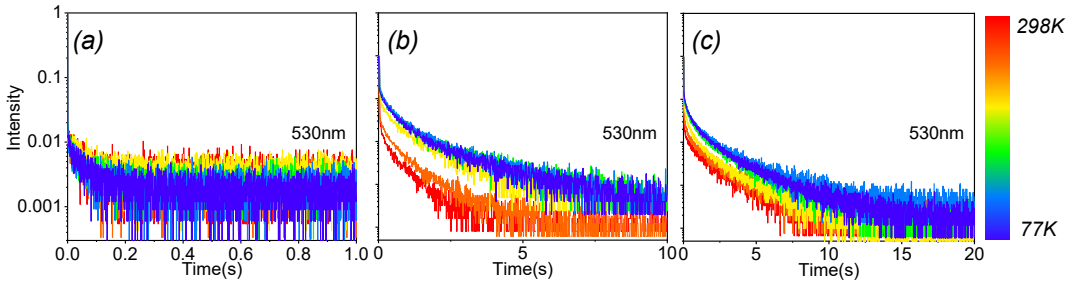

Fig. S3 Temperature dependence transient PL decay spectra from 298 K to 77 K of crystal, (a) OID, (b) OID-6, (c) OID-7.

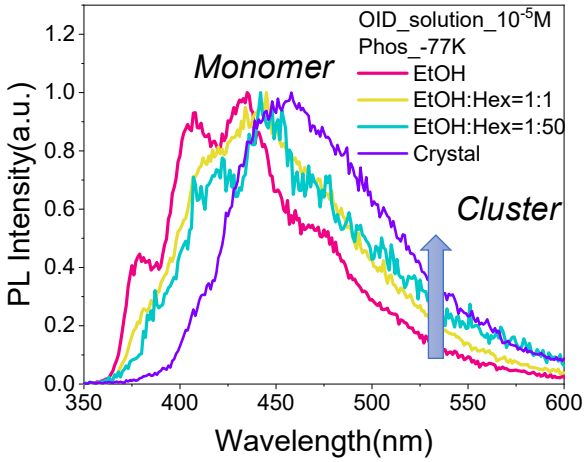

Fig. S4 PL spectra of the of OID 10^{-5} M solution with different ratios of EtOH: Hex and PL spectra of OID crystal.

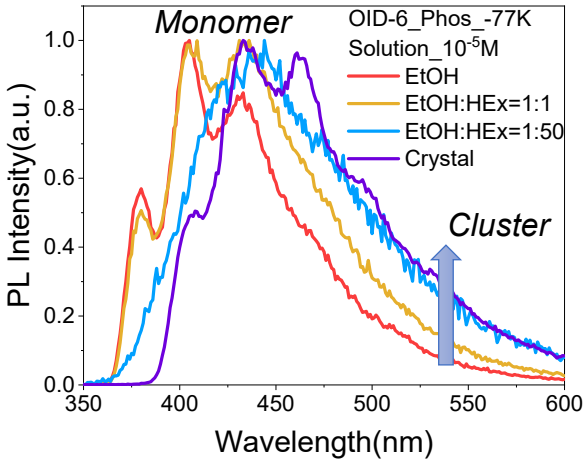

Fig. S5 PL spectra of the OID-6 10^{-5} M solution with different ratios of EtOH: Hex and PL spectra of OID-6 crystal.

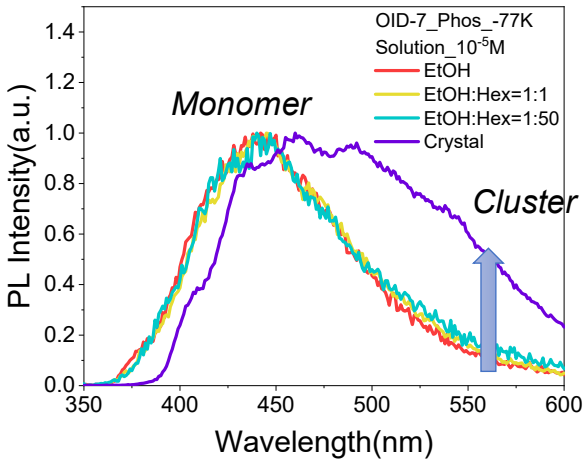

Fig. S6 PL spectra of the OID-7 10^{-5} M solution with different ratios of EtOH: Hex and PL spectra of OID-7 crystal.

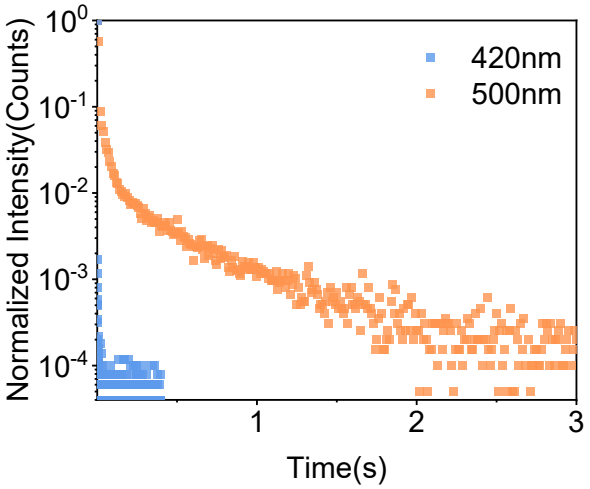

Fig. S7 Transient PL decay spectra of the OID crystal at different wavelengths.

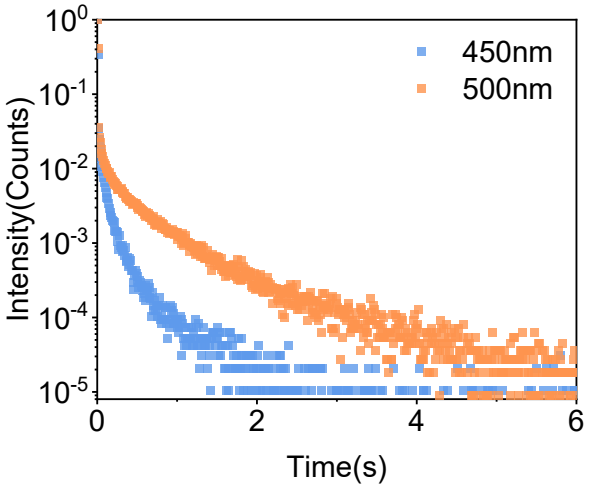

Fig. S8 Transient PL decay spectra of the OID-6 crystal at different wavelengths.

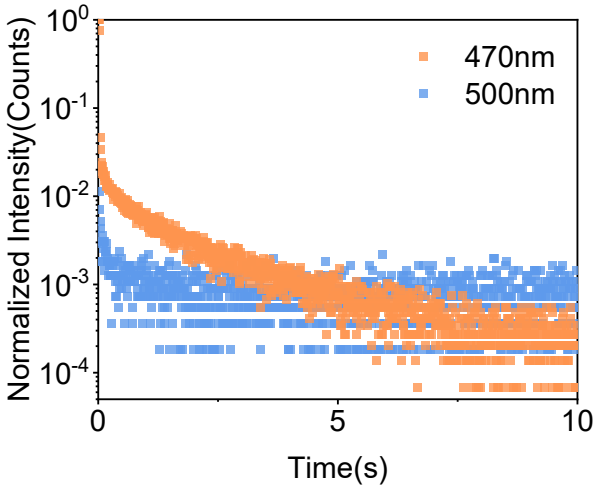

Fig. S9 Transient PL decay spectra of the OID-7 crystal at different wavelengths.

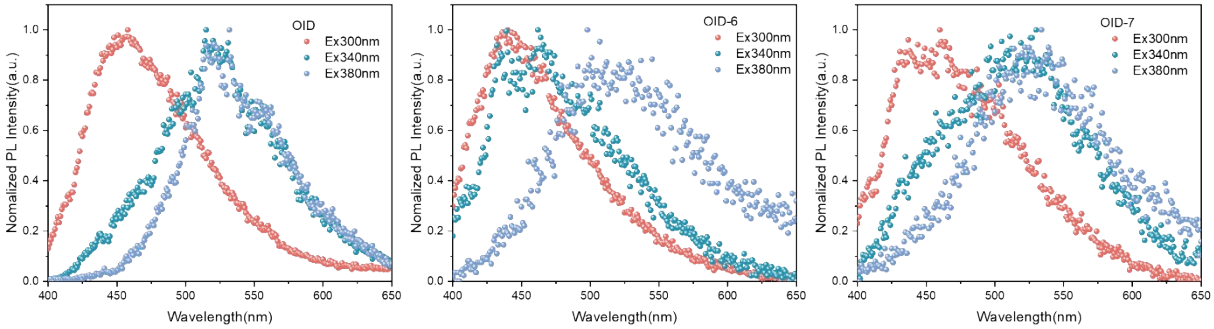

Fig. S10 Phosphorescence spectra with different excitation wavelengths

Table S1. Photophysical properties of the three compounds in crystalline state.

	$\Phi_F{}^a$ (%)	$\Phi_P{}^a$ (%)	$\Phi_{P,s}{}^{a,b}$ (%)	$\Phi_{P*}{}^{a,c}$ (%)	k_F (s^{-1})	k_{P*} (s^{-1})	$k_{isc}+k_{ic}$ (s^{-1})	$K_{vnr}+k_q{}^d$ (s^{-1})
OID	2.47	4.83	2.25	2.58	6.02×10^{6}	7.32×10^{-2}	2.38×10^{8}	2.77
OID-6	2.96	5.25	3.91	1.34	1.26×10^{7}	2.62×10^{-2}	4.11×10^{8}	1.92
OID-7	3.58	6.58	4.27	2.31	1.86×10^{7}	1.42×10^{-2}	5.02×10^{8}	0.60

*$k_F=\Phi_F/\tau_F$, $k_{P*}=\Phi_{P*}/\tau_{P*}$, $k_{isc}+k_{ic}=(1-\Phi_F)/\tau_F$, $k_{vnr}+k_q=(1-\Phi_P{}^*)/\tau_P{}^*$

*a, Φ_F, $\Phi_{P,s}$ and $\Phi_P{}^*$ were derived from their prompt and delayed emission spectra.

b, Phosphorescence quantum yield of the compound in isolated state.

c, Phosphorescence quantum yield of the compound in cluster state.

d, Non-radiative rate of intramolecular vibrational relaxation and triplet quenching from cluster triplet state.

2.2 ONIOM model and computation details

Cluster structures were extracted from single crystal XRD results. The clusters used for computation were chosen as a central molecule with its surrounding molecules within one molecule. In the ONIOM model, the central molecule was chosen as high layer using quantum methods in B3lyp(d3)/6-311g* level and the surrounding molecules as low layer using PM7. Then the excited state energies were calculated using TD-DFT. And the surrounding molecules were replaced by RESP electrons.

And as shown in Fig. S11, the calculated phosphorescence wavelength based on the T_1 excited state geometries using ONIOM method to simulate the cluster environment were corresponding well with the phosphorescence spectra of crystal which could further prove the delayed emissions located at the shorter wavelength were radiated from single molecular triplet states.

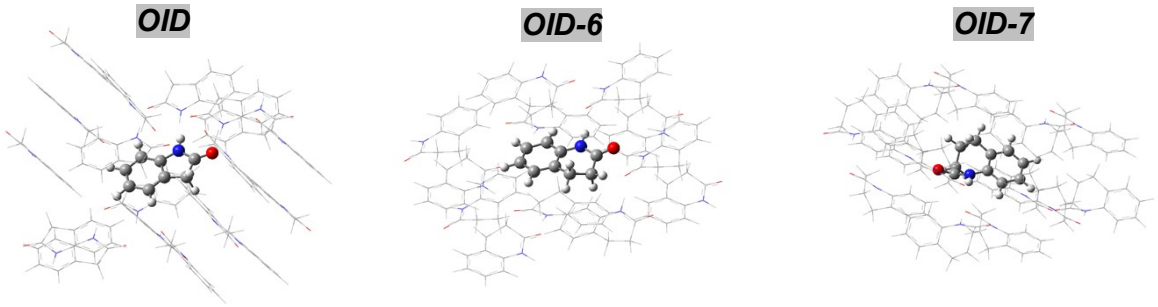

Fig. S11 ONIOM models of OID, OID-6 and OID-7 clusters.

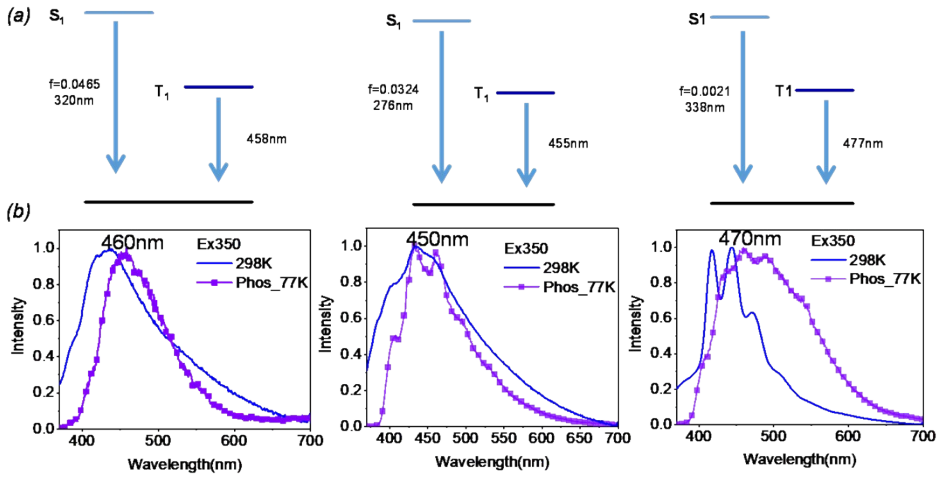

Fig. S12 (a) The calculated energy diagrams of OID, OID-6 and OID-7 using ONIOM method based on T_1 excited state geometries, (b) Steady state PL spectra and phosphorescence spectra of OID, OID-6 and OID-7 crystal.

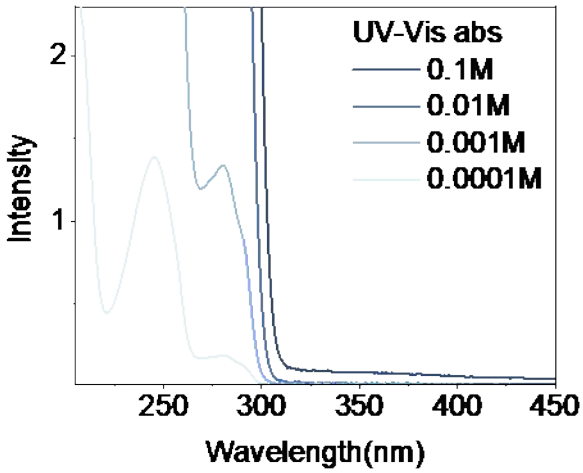

Fig. S13 UV-vis absorption spectra of OID in CH_3CN solution of different concentrations.

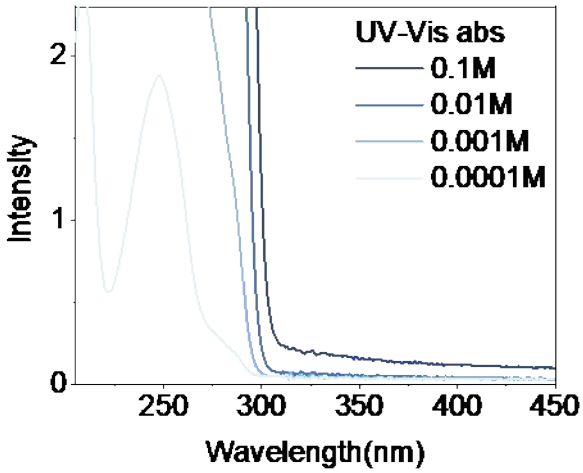

Fig. S14 UV-vis absorption spectra of OID-6 in CH_3CN solution of different concentrations.

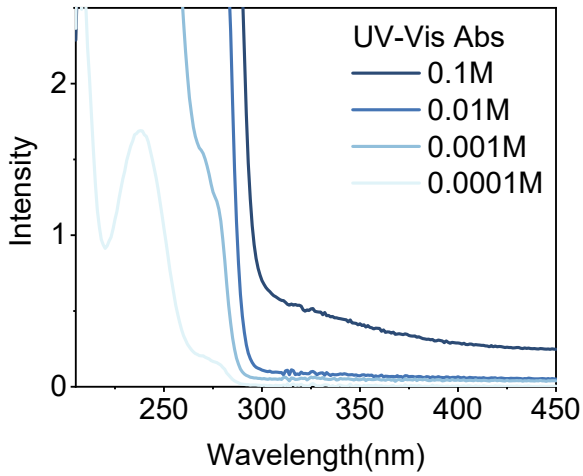

Fig. S15 UV-vis absorption spectra of OID-7 in CH_3CN solution of different concentrations.

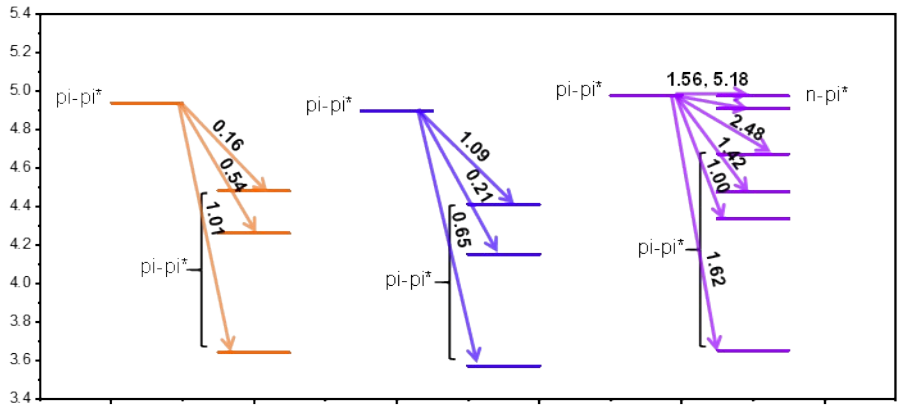

Fig. S16 Calculated energy diagrams of OID, OID-6 and OID-7 based on S_0 geometries and the SOC between S_1 and T_n.

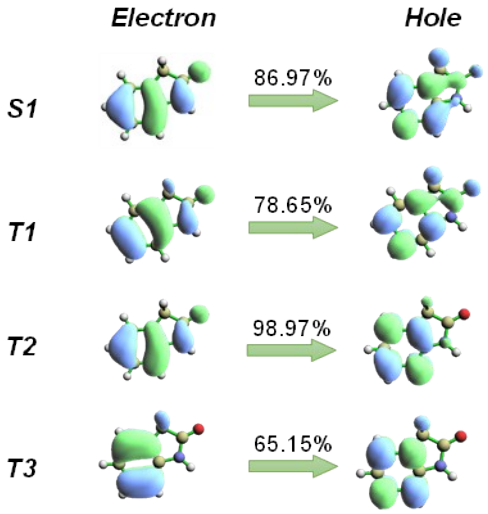

Fig. S17 NTOs of singlet and triplet states of OID.

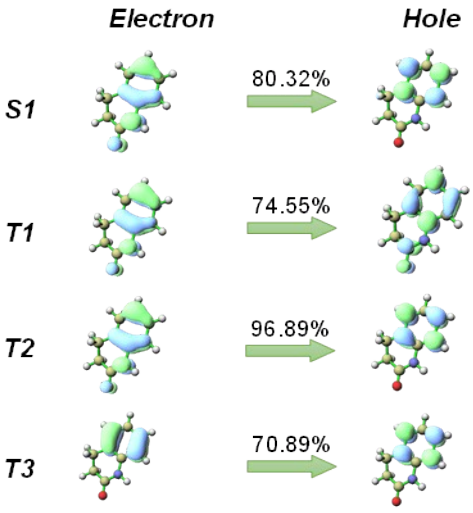

Fig. S18 NTOs of singlet and triplet states of OID-6.

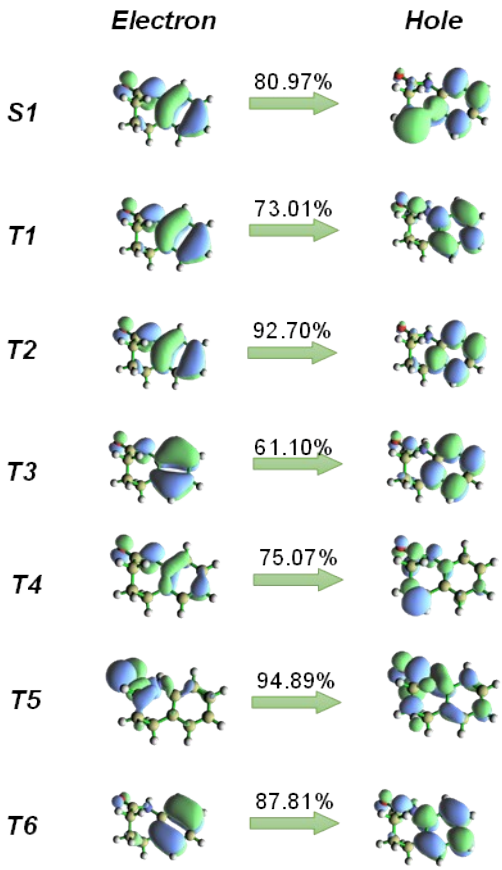

Fig. S19 NTOs of singlet and triplet states of OID-7.

2.3 Relationship between triplet exciton diffusion and overlap between FMOs

In the previous report, Hirata et. al. demonstrated that small overlap between the FMOs could prevent triplet excitons from diffusing over a long distance and consequently from quenching at defect sites inside the crystal or at the crystal surface.[10-12] As shown in the Equation S1 and S2, the triplet exciton diffusion coefficient at RT (***D*$_t$ *(RT)***) is proportional to the electron transfer rate at RT ($k_{et}(RT)$)and the hole transfer rate at RT ($k_{h_t}(RT)$). And $k_{et}(RT)$ and $k_{h_t}(RT)$ can be expressed in the frame of Marcus theory (Equation.S2) where $t^2_{et(ht)}$ is the transfer integral of electron transfer (hole transfer). And $t^2_{et(ht)}$ is related to the overlap between FMOs. Therefore, small overlaps between FMOs could prevent triplet exciton from diffusing and consequently from quenching.

$$D_t(RT) \propto k_{et}(RT) k_{h_t}(RT) \qquad \textbf{Equation.S1}$$

$$k_{et(h_t)} = \frac{t^2_{et(ht)}}{\hbar}\sqrt{\frac{\pi}{\lambda k_B T}}\exp\left(\frac{-\lambda_{et}(ht)}{4k_B T}\right) \qquad \textbf{Equation.S2}$$

2.4 Single crystal analysis

Table S1. Crystal information of the three compounds

Name	OID	OID-6	OID-7
Formula	C_8H_7NO	C_9H_9NO	$C_{10}H_{11}NO$
Space group	P 2_1/c	P 2_1 2_1 2_1	P 1
Cell length (Å)	**a** 12.791	**a** 7.5949	**a** 8.892
	b 8.1237	**b** 7.59466	**b** 9.5749
	c 13.4636	**c** 12.7739	**c** 11.0673
Cell angles (°)	**a** 90	**a** 90	**a** 88.161
	b 111.515	**b** 90	**b** 72.351
	g 90	**g** 90	**g** 68.649
Cell Volume(Å^3)	1301.53	736.807	833.032
Z	**8**	**4**	**4**

3. Materials details

OID, OID-6 and OID-7 were purchased from commercial source and were further purified using column chromatography with petroleum ether and dichloromethane and recrystallized three times using ethanol to ensure the purity.

Indolin-2-one (OID)

^{1}H NMR (500 MHz, Chloroform-*d*) δ 9.43 (s, 1H), 7.22 (d, *J* = 7.5 Hz, 2H), 7.10 – 6.81 (m, 2H), 3.54 (s, 2H). ^{13}C NMR (101 MHz, Chloroform-*d*) δ 178.32, 142.65, 127.95, 125.34, 124.60, 122.36, 109.89, 36.42. HRMS(ESI+) m/z Calcd for C8H7NO+Na$^+$: 156.0420; found: 156.0428.

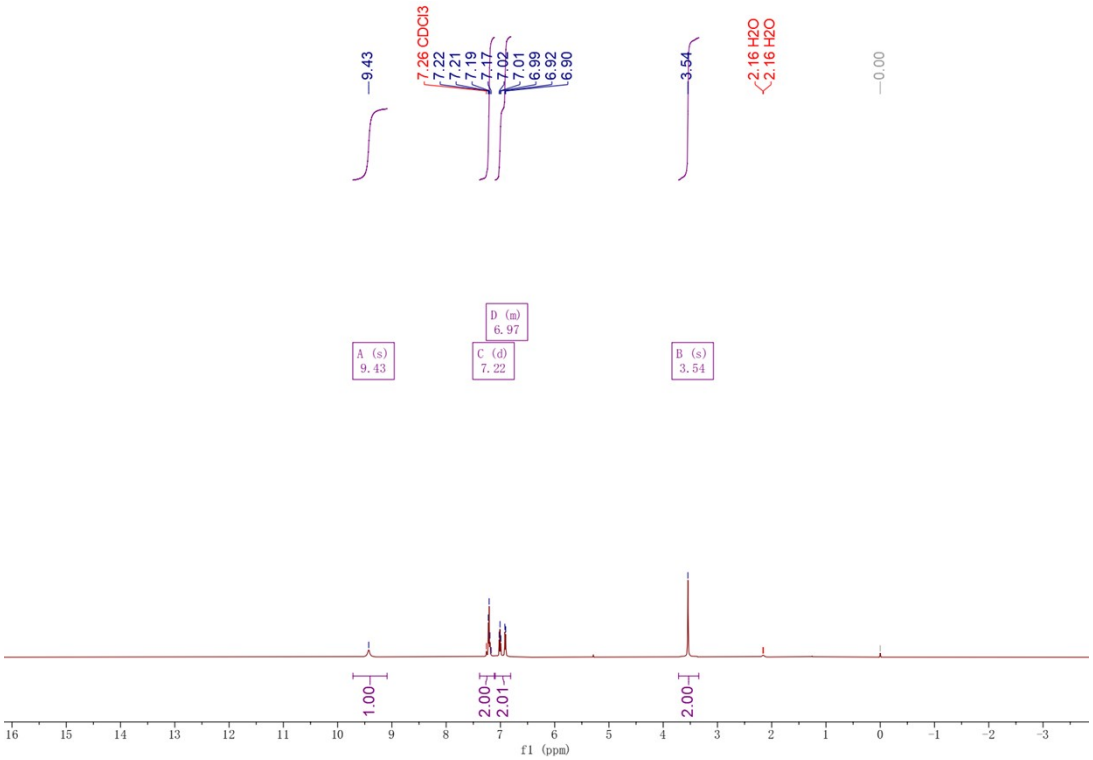
9.43
7.26 CDCl3
7.22
7.21
7.19
7.17
7.02
7.01
6.99
6.92
6.90
3.54
2.16 H2O
2.16 H2O
0.00
D (m)
6.97
A (s)
9.43
C (d)
7.22
B (s)
3.54
1.00
2.00
2.01
2.00
f1 (ppm)

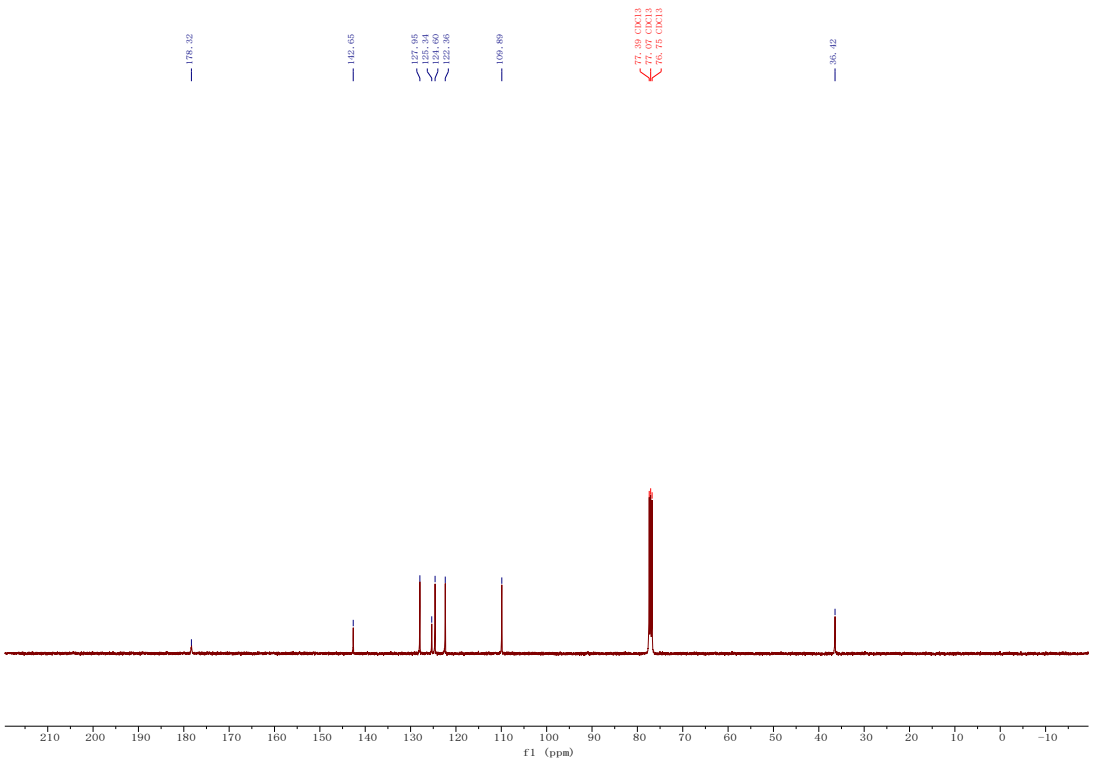
178.32
142.65
127.95
125.14
123.60
122.36
109.89
77.39 CDCl3
77.07 CDCl3
76.75 CDCl3
36.42
f1 (ppm)

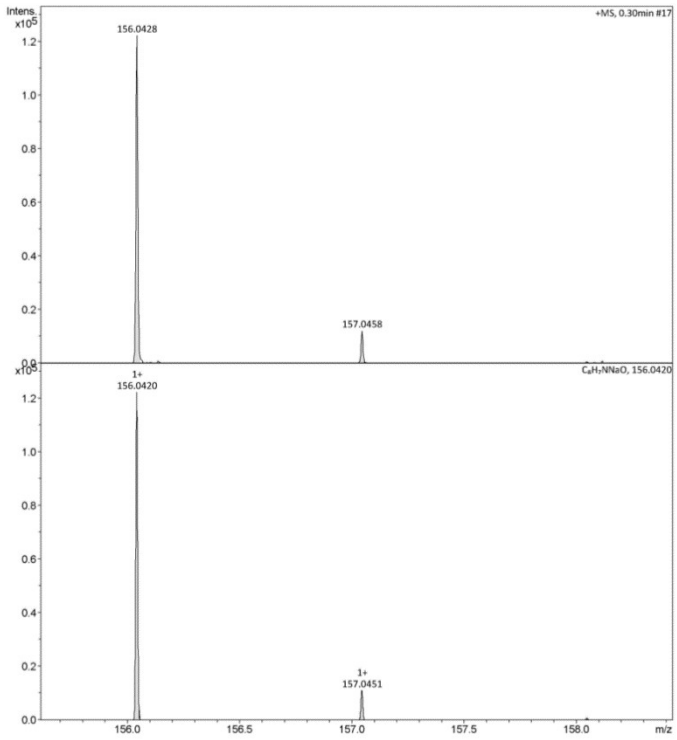

Fig.S20 ^{1}H and ^{13}C NMR spectra and HRMS spectrum of OID.

3,4-dihydroquinolin-2(1H)-one (OID-6)

^{1}H NMR (500 MHz, Chloroform-*d*) δ 9.19 (s, 1H), 7.17 (ddd, *J* = 11.3, 7.6, 2.7 Hz, 2H), 6.98 (t, *J* = 7.4 Hz, 1H), 6.85 (d, *J* = 7.8 Hz, 1H), 2.97 (t, *J* = 7.6 Hz, 2H), 2.65 (dd, *J* = 8.5, 6.6 Hz, 2H). ^{13}C NMR (101 MHz, Chloroform-*d*) δ 172.34, 137.33, 127.92, 127.55, 123.64, 123.09, 115.60, 30.74, 25.33. HRMS(ESI+) m/z Calcd for C9H10NO+H^{+}: 148.0757; found: 148.0766.

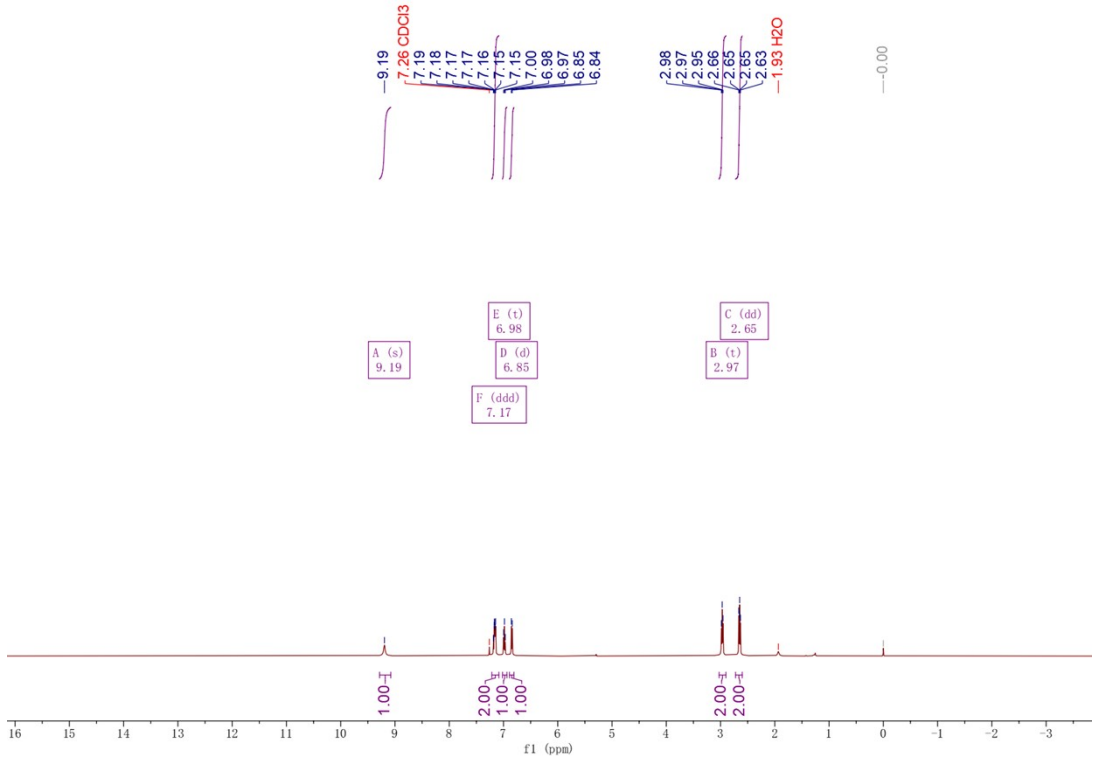

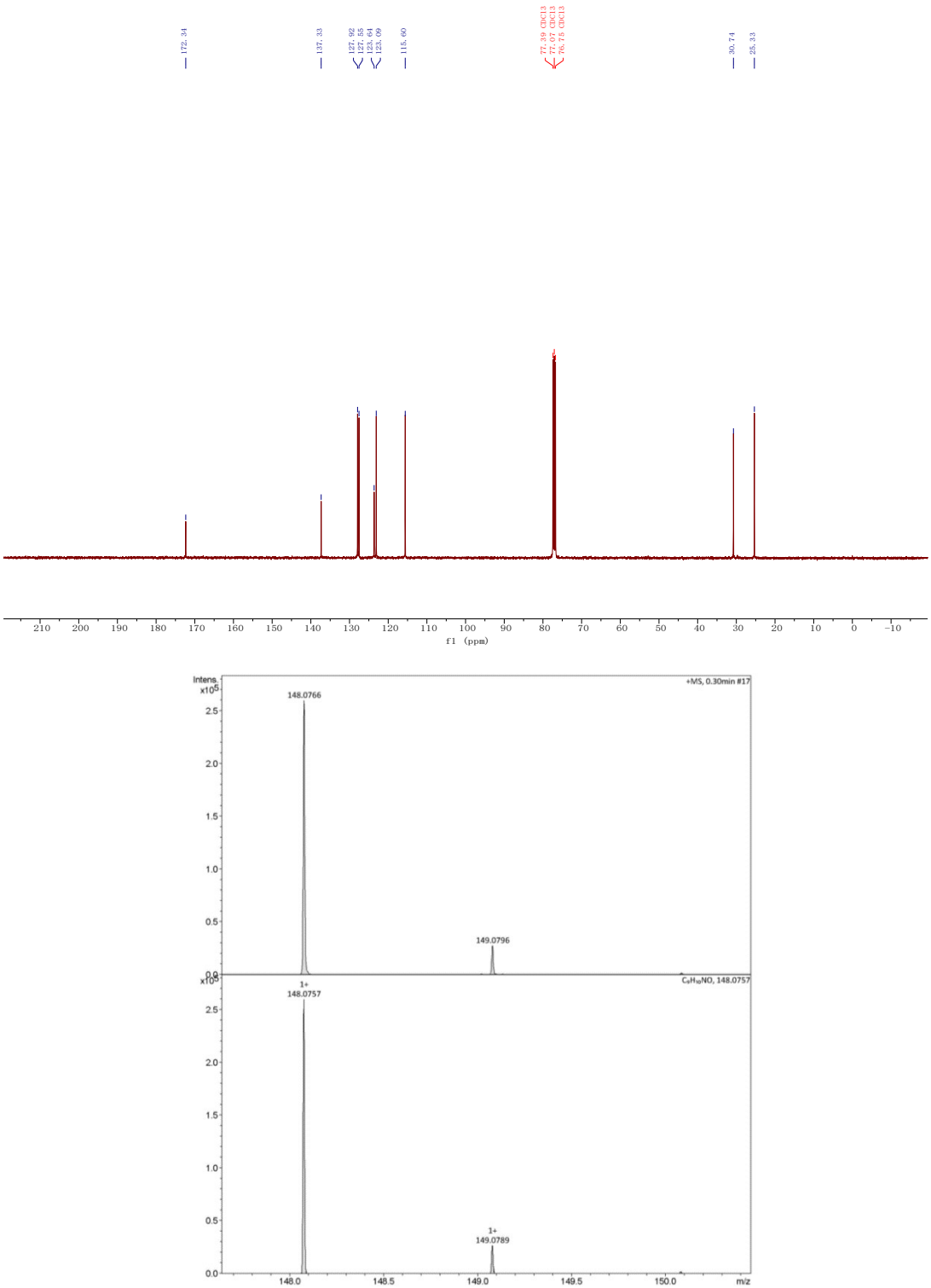

Fig.S21 ^{1}H and ^{13}C NMR spectra and HRMS spectrum of OID-6.

1,3,4,5-tetrahydro-2H-benzo[b]azepin-2-one (OID-7)

^{1}H NMR (500 MHz, Chloroform-*d*) δ 8.46 (s, 1H), 7.26 – 7.19 (m, 2H), 7.13 (td, *J* = 7.5, 1.3 Hz, 1H), 7.04 – 6.99 (m, 1H), 2.80 (t, *J* = 7.2 Hz, 2H), 2.37 (t, *J* = 7.3 Hz, 2H), 2.24 (t, *J* = 7.3 Hz, 2H). ^{13}C NMR (126 MHz, Chloroform-*d*) δ 175.61, 137.93, 134.29, 129.82, 127.47, 125.63, 121.86, 32.80, 30.33, 28.55. HRMS(ESI+) m/z Calcd for C10H12NO+Na^{+}: 162.0913; found: 162.0922.

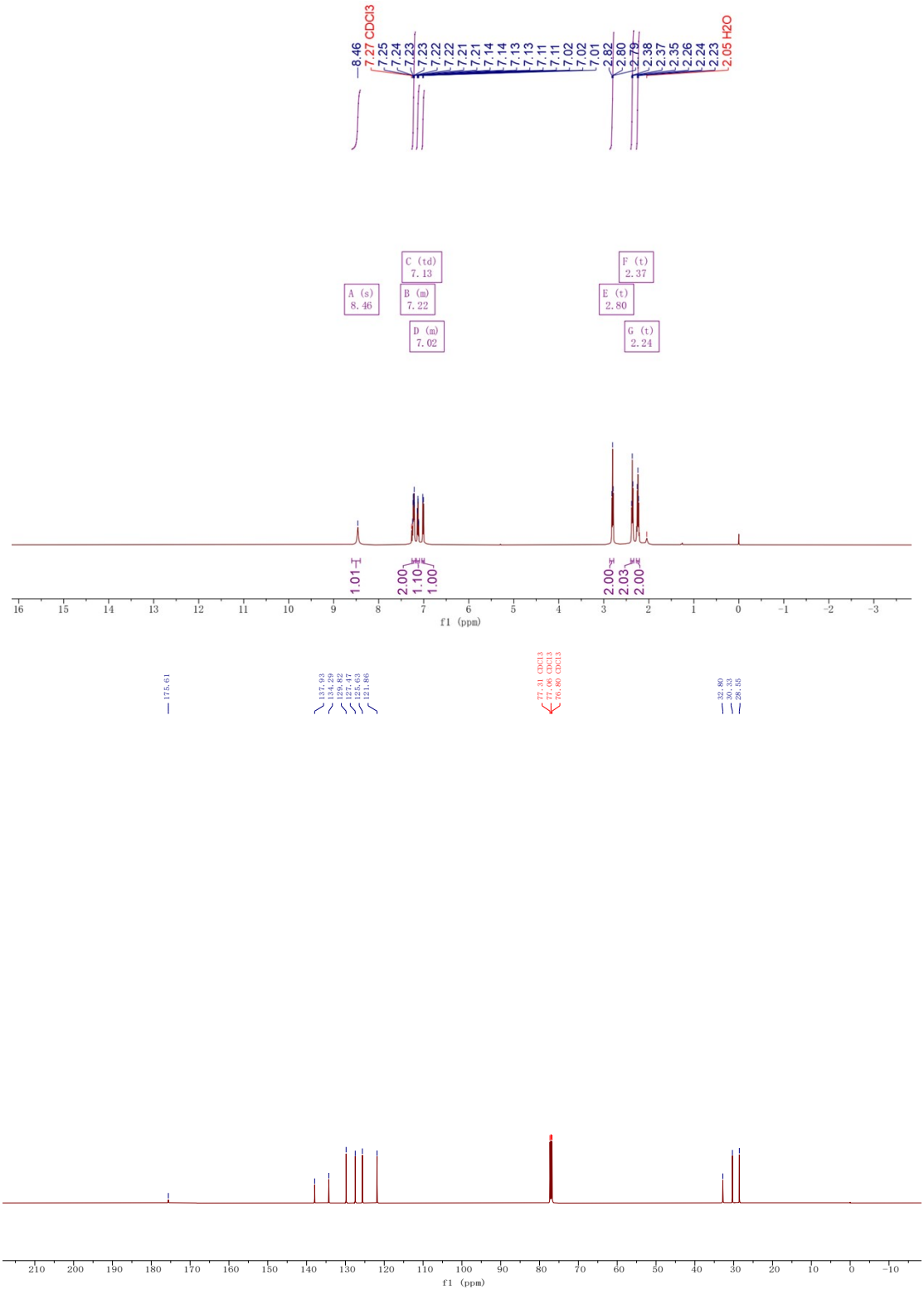
8.46
7.27 CDCl3
7.25
7.24
7.23
7.23
7.22
7.22
7.21
7.21
7.14
7.14
7.13
7.13
7.11
7.11
7.02
7.02
7.01
2.82
2.80
2.79
2.38
2.37
2.35
2.26
2.24
2.23
2.05 H2O
A (s) 8.46
C (td) 7.13
B (m) 7.22
D (m) 7.02
F (t) 2.37
E (t) 2.80
G (t) 2.24
1.01
2.00
1.10
1.00
2.00
2.03
2.00
f1 (ppm)
175.61
137.93
134.29
129.82
127.47
125.63
121.86
77.31 CDCl3
77.06 CDCl3
76.80 CDCl3
32.80
30.33
28.55
f1 (ppm)

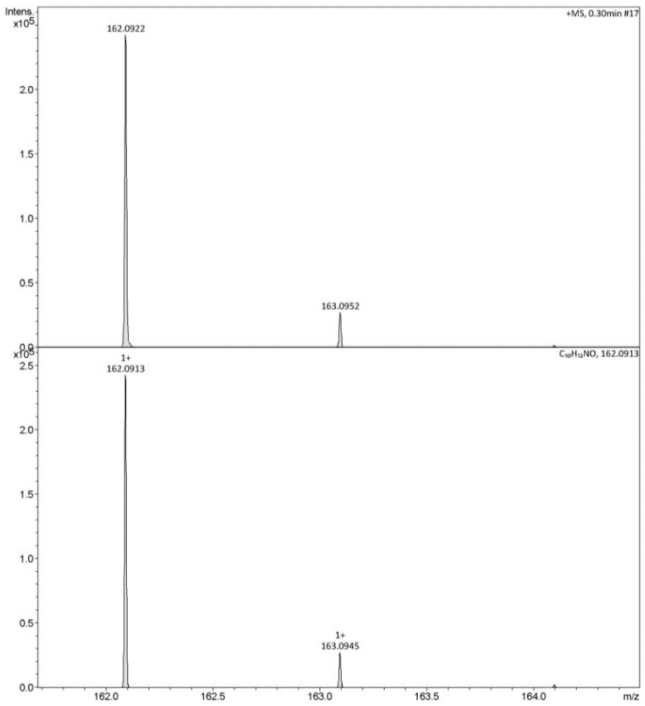

Fig.S22 ^{1}H and ^{13}C NMR spectra and HRMS spectrum of OID-7.

Purity of the sample for measurement:

To further verify their purity and exclude the impact of impurity, the crystal samples were grinded into powder for comparison and dissolved into dichloromethane solution with further column chromatography and recrystallization with ethanol. Before and after column chromatography and recrystallization, they all exhibited identical single spot in the thin liquid chromatography (TLC) under 254 nm irradiation with dichloromethane as eluent (Fig. S23), and their RTP spectra of powder were also identical (Fig. S24).

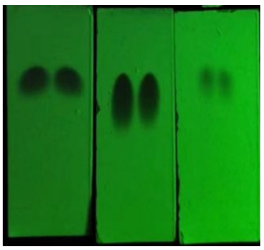

OID OID-6 OID-7

Fig. S23. Photograph of TLC spots when irradiated at 254 nm before and after a further purification of column chromatography using silica gels and recrystallization.

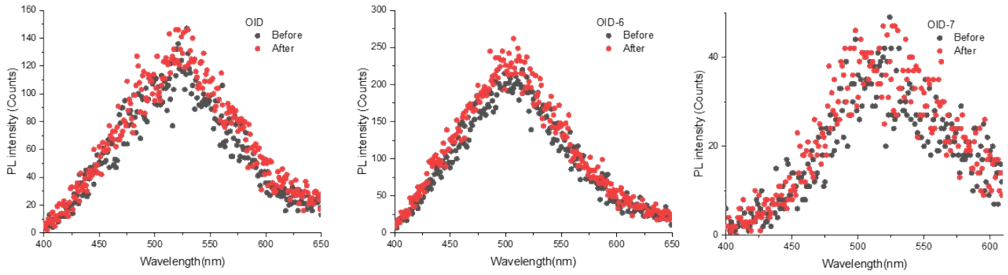

Fig. S24. RTP spectra of powders before and after further purification.

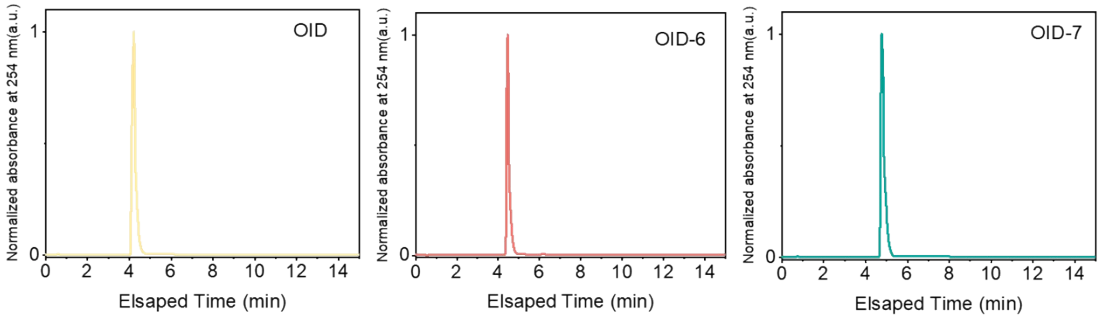

Fig. S25. HPLC diagrams of OID, OID-6 and OID-7.

References:

1. R. A. Gaussian 09, M. J. Frisch, G. W. Trucks, H. B. Schlegel, G. E. Scuseria, M. A. Robb, J. R. Cheeseman, G. Scalmani, V. Barone, G. A. Petersson, H. Nakatsuji, X. Li, M. Caricato, A. V. Marenich, J. Bloino, B. G. Janesko, R. Gomperts, B. Mennucci, H. P. Hratchian, J. V. Ortiz, A. F. Izmaylov, J. L. Sonnenberg, Williams, F. Ding, F. Lipparini, F. Egidi, J. Goings, B. Peng, A. Petrone, T. Henderson, D. Ranasinghe, V. G. Zakrzewski, J. Gao, N. Rega, G. Zheng, W. Liang, M. Hada, M. Ehara, K. Toyota, R. Fukuda, J. Hasegawa, M. Ishida, T. Nakajima, Y. Honda, O. Kitao, H. Nakai, T. Vreven, K. Throssell, J. A. Montgomery Jr., J. E. Peralta, F. Ogliaro, M. J. Bearpark, J. J. Heyd, E. N. Brothers, K. N. Kudin, V. N. Staroverov, T. A. Keith, R. Kobayashi, J. Normand, K. Raghavachari, A. P. Rendell, J. C. Burant, S. S.

Iyengar, J. Tomasi, M. Cossi, J. M. Millam, M. Klene, C. Adamo, R. Cammi, J. W. Ochterski, R. L. Martin, K. Morokuma, O. Farkas, J. B. Foresman and D. J. Fox, Gaussian, Inc., Wallingford CT, 2016.
2. E. Runge and E. K. U. Gross, *Phys. Rev. Lett.*, 1984, **52**, 997-1000.
3. P. J. Stephens, F. J. Devlin, C. F. Chabalowski and M. J. Frisch, *J. Phys. Chem. C*, 2002, **98**, 11623-11627.
4. A. Dreuw and M. Head-Gordon, *Chem. Rev.*, 2005, **105**, 4009-4037.
5. C. I. Bayly, P. Cieplak, W. Cornell and P. A. Kollman, *J. Phys. Chem. C*, 2002, **97**, 10269-10280.
6. C. Lefebvre, G. Rubez, H. Khartabil, J. C. Boisson, J. Contreras-Garcia and E. Henon, *Phys. Chem. Chem. Phys.*, 2017, **19**, 17928-17936.
7. W. Humphrey, A. Dalke and K. Schulten, *J. Mol. Graph. Model.*, 1996, **14**, 33-38.
8. T. Lu and F. Chen, *J. Comput. Chem.*, 2012, **33**, 580-592.
9. X. Gao, S. Bai, D. Fazzi, T. Niehaus, M. Barbatti and W. Thiel, *J. Chem. Theory Comput.*, 2017, **13**, 515-524.
10. S. Hirata, *J. Mater. Chem. C*, 2018, **6**, 11785-11794.
11. S. Hirata, K. Totani, J. Zhang, T. Yamashita, H. Kaji, S. R. Marder, T. Watanabe and C. Adachi, *Adv. Funct. Mater.*, 2013, **23**, 3386-3397.
12. K. Narushima, Y. Kiyota, T. Mori, S. Hirata and M. Vacha, *Adv. Mater.*, 2019, **31**, e1807268.